Supporting Information

Tumor marker detection with surface enhanced Raman spectroscopy on 3D Au butterfly wings

Guofen Song,[a] Han Zhou,[a] Jiajun Gu,[a] Qinglei Liu,[a] Wang Zhang,[a] Huilan Su,[a] Yishi Su,[a] Qinghua Yao*[b] and Di Zhang*[a]*

[a] State Key Laboratory of Metal Matrix Composites, Shanghai Jiao Tong University, Shanghai 200240, China. *E-mail: gujiajun@sjtu.edu.cn; zhangdi@sjtu.edu.cn; Tel: +86-21-34202634

[b] Key Laboratory of Integrated Traditional Chinese and Western Medicine, Department of Integrated Traditional Chinese and Western Medicine, Zhejiang Cancer Hospital, Hangzhou, Zhejiang 310053, China. *E-mail: yaoqh@zjcc.org.cn

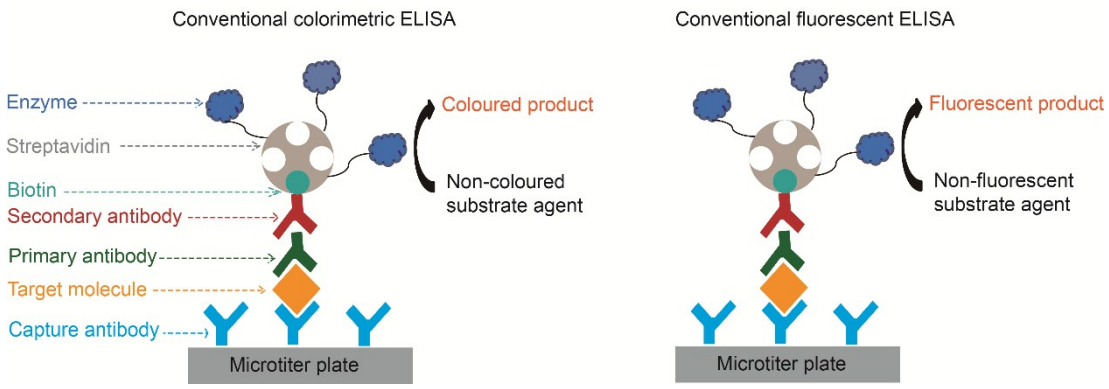

Fig. S1. Schematic illustration of conventional ELISA. In this sandwich ELISA the target molecule is anchored to the substrate plate by capture antibodies and recognized by primary antibodies. The enzyme is linked to the immunocomplex through interactions between biotinylated secondary antibodies and enzyme-decorated streptavidin. In conventional colorimetric ELISA, enzymatic biocatalysis generates a colored or fluorescent compound.

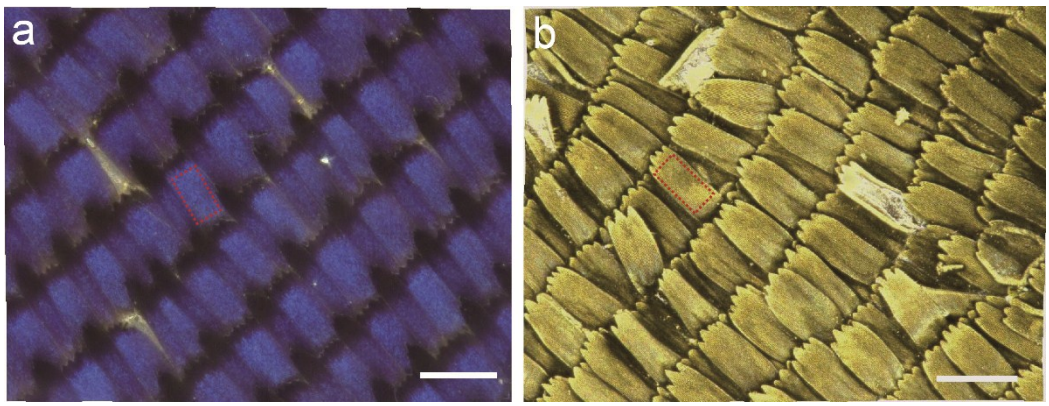

Fig. S2. Optical microscopy images of original *E. mulciber* dorsal forewing (a) and the corresponding Au replica (b). Scale bar: 100 μm. The Raman signals were acquired within the red rectangular area of wing scales.

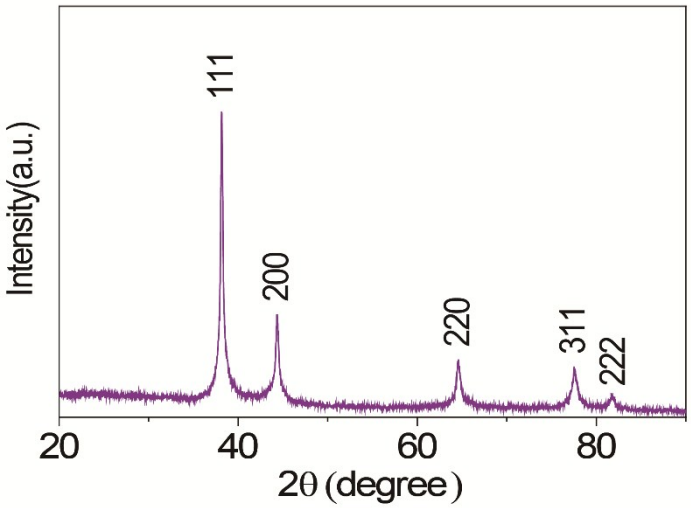

Fig. S3. XRD results of Au BWs.

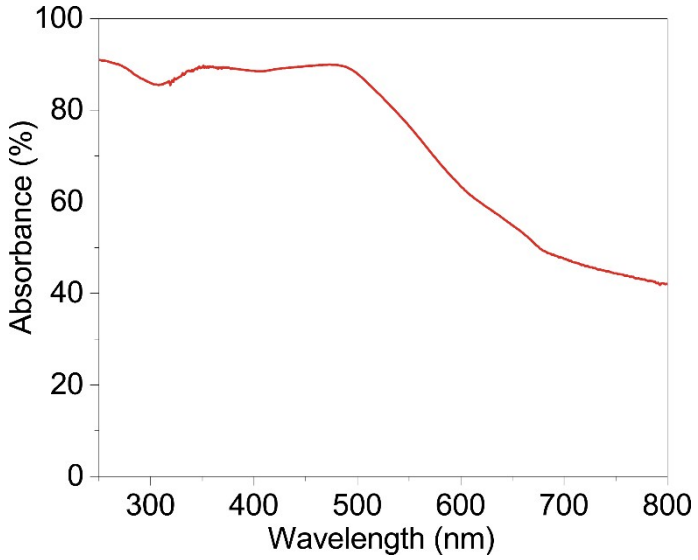

Fig. S4. Absorbance spectrum of Au BWs.

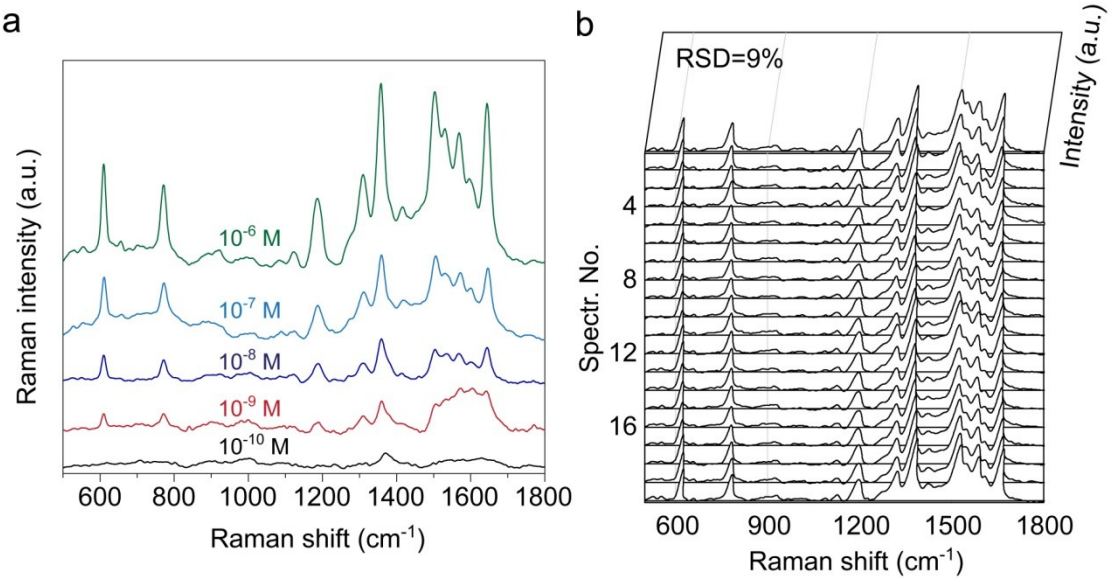

Fig. S5. Raman spectra of R6G on Au BWs. (a) Raman signals of a series of concentrations from 10^{-10} M to 10^{-6} M R6G on Au BWs. (b) Raman signals acquired at 20 randomly chosen spots from 10 Au scales for reproducibility evaluation (10^{-6} M).

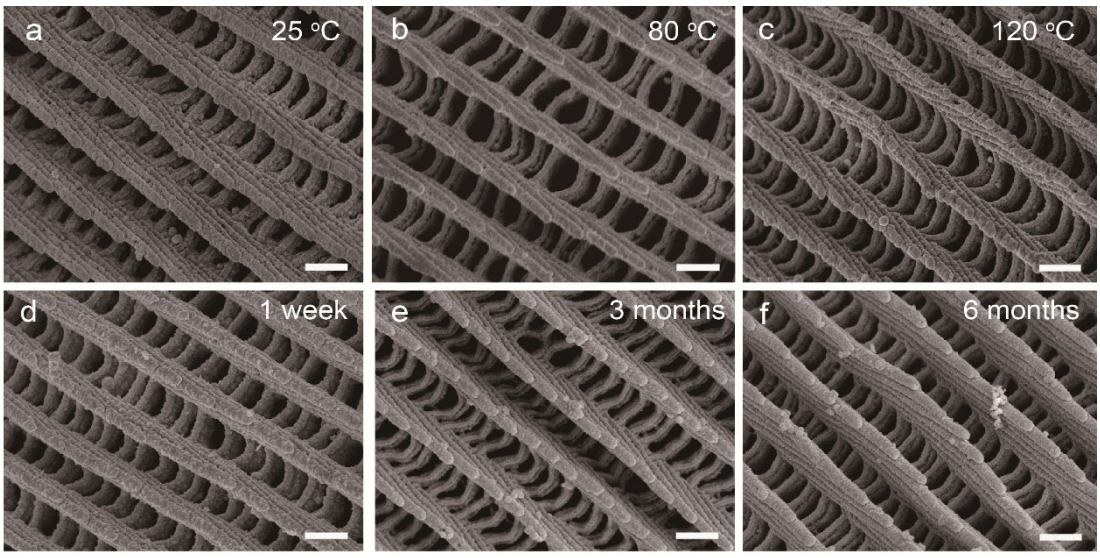

Fig. S6. Stability of the Au butterfly wings. (a)–(c) Lower magnification SEM images of Au BWs incubated at 25, 80, and 120 ºC for 2 h; (d)–(f) Au BWs stored for 1 week, 3 and 6 months at room temperature, respectively. Scale bars: 1 μm.

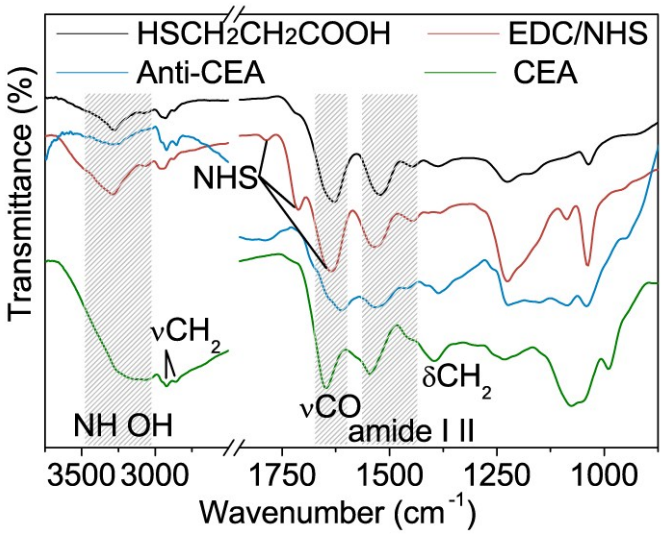

Fig. S7. FTIR-ATR spectra of Q-SERS (commercial substrates) functionalized with $HSCH_2CH_2COOH$, EDC/NHS, anti-CEA, and CEA in sequence.

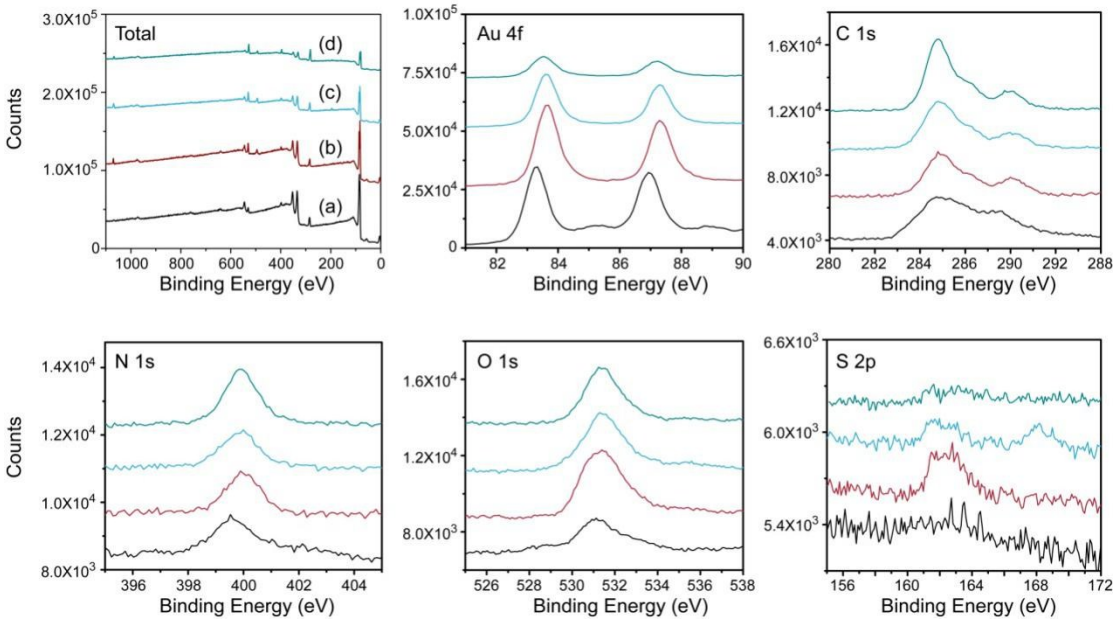

Fig. S8. XPS spectra of Au BWs functionalized with (a) ethanol, (b) $HSCH_2CH_2COOH$, (c) anti-CEA, and (d) CEA in sequence.

Table S1. Binding energy (eV) and compositional assignments from the XPS spectra of the Au BWs treated via $HSCH_2CH_2COOH$, anti-CEA, and CEA in sequence.

Elements	Binding energy (eV)			
	Au BWs	$HSCH_2CH_2COOH$	Anti-CEA	CEA
Au 4f	83.3	83.7	83.7	83.6
S 2p	/	162.1, 163.0	162.0, 163.0	161.6, 163.6
C 1s	284.7	284.8, 288.0	284.8, 288.0	284.8, 288.0
N 1s	399.5	400.1	400.0	400.0
O 1s	531.7	531.4, 531.5	531.3, 531.5	531.2, 531.5

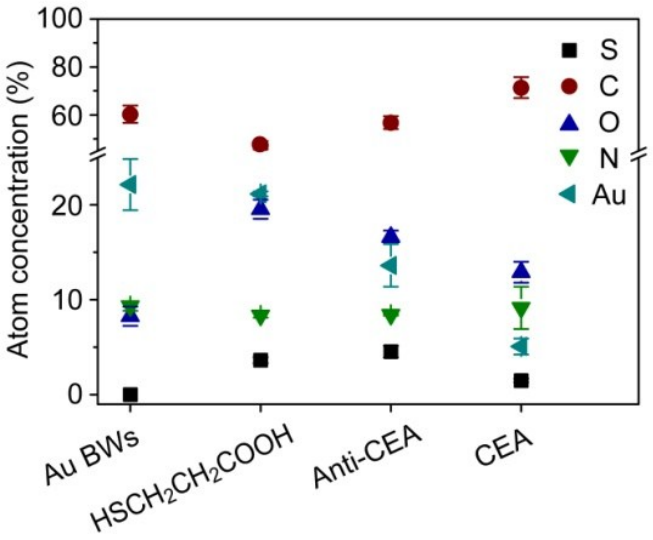

Fig. S9. Atom concentration of Au, N, O, C, and S from XPS spectra of the Au BWs treated via $HSCH_2CH_2COOH$, anti-CEA, and CEA in sequence.

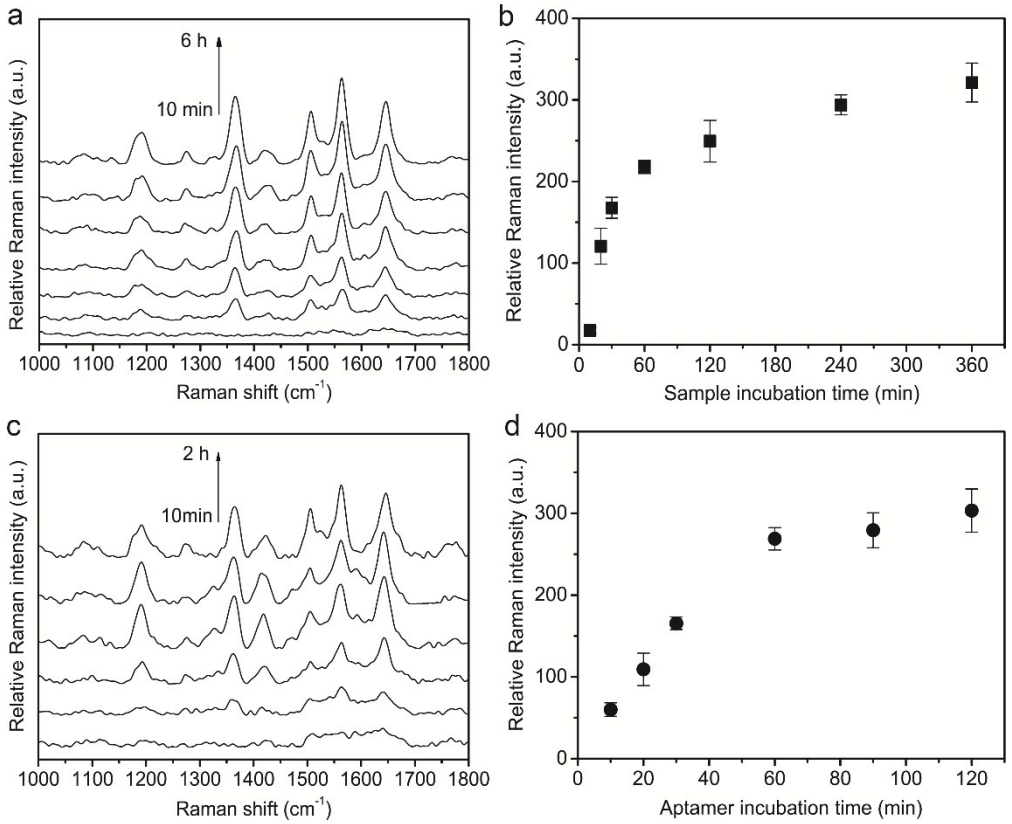

Fig. S10. Raman signal at different detection conditions. a and b: different sample incubation time of 10min, 30min, 1h, 1.5h, 2h, 4h and 6h (from bottom to top); c and d: different aptamer incubation time of 10min, 30min, 1h, 1.5h and 2h (from bottom to top).

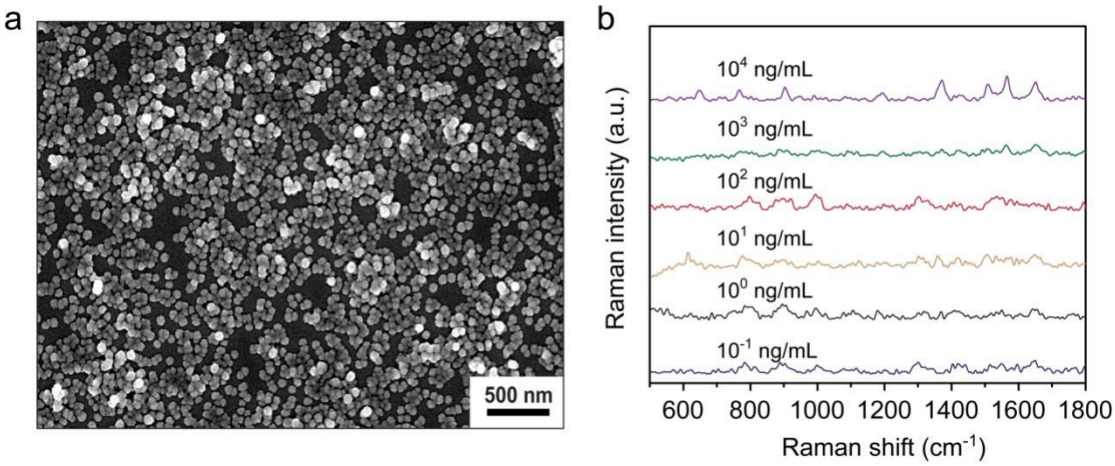

Fig. S11. (a) SEM image of the surface texture of the commercial Q-SERS substrate. (b) Raman spectra of a series of CEA samples with various concentrations collected on the Q-SERS. The substrate was treated via the same method shown in Scheme 1 in the main text.

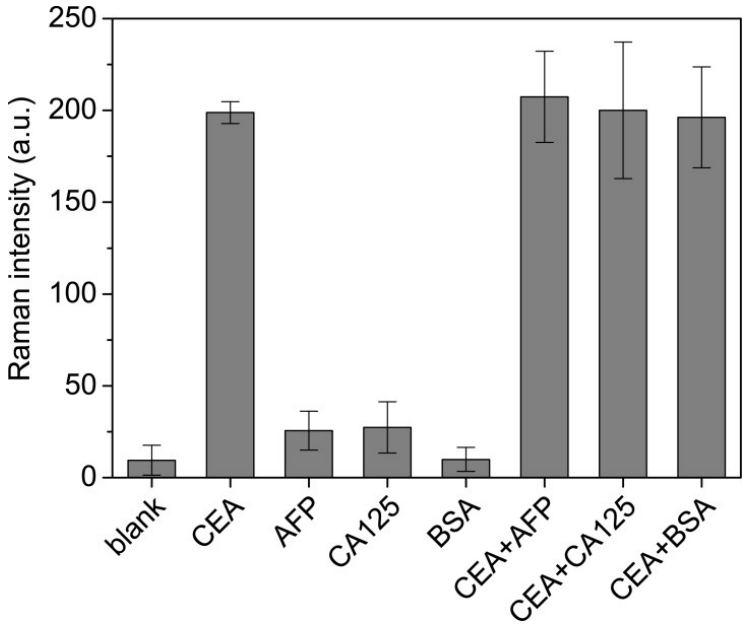

Fig. S12. The recognition specificity of functionalized Au BWs for CEA: CEA (100 ng/mL), AFP (1000 ng/mL), CA125 (1000 ng/mL) and BSA (1000 ng/mL).